HIV-1 Reverse Transcriptase Can Discriminate between Two Conformationally Locked Carbocyclic AZT Triphosphate Analogues

Victor E. Marquez,*,† Abdallah Ezzitouni,† Pamela Russ,† Maqbool A. Siddiqui,† Harry Ford, Jr.,† Ron J. Feldman,‡ Hiroaki Mitsuya,‡ Clifford George,§ and Joseph J. Barchi, Jr.†

Contribution from the Laboratory of Medicinal Chemistry, Division of Basic Sciences, and Experimental Retrovirology Section, Medicine Branch, Division of Clinical Sciences, National Cancer Institute, National Institutes of Health, Bethesda, Maryland 20892, and Laboratory for the Structure of Matter, Naval Research Laboratory, Washington, D.C. 20375

Received October 8, 1997

Abstract: It has been proposed that the preference of 3′-azido-3′-deoxythymidine (AZT) for the extreme $_3E$ (south) conformation, as observed in its X-ray structure, is responsible for its potent anti-HIV activity. However, it has also been suggested that the antipodal north conformation may be required for the strong interaction of AZT 5′-triphosphate with its target enzyme, HIV reverse transcriptase (RT). To resolve this issue, we have constructed two conformationally rigid carbocyclic analogues of AZT which are locked permanently into opposite $_2E$ (north) and $_3E$ (south) conformations in order to test the ability of the corresponding 5′-triphosphates to inhibit RT. The two isomeric carbocyclic analogues of AZT, (N)-*methano*-carba-AZT (**1**) and (S)-*methano*-carba-AZT (**2**), were constructed on a bicyclo[3.1.0]hexane template that exhibits a rigid pseudoboat conformation, capable of mimicking the furanose pucker in the classical north and south conformations that are characteristic of standard nucleosides. The unique conformational properties of **1** and **2** observed by both X-ray and solution NMR studies showed the existence of the same invariant conformations in solution and in the solid state. In addition, differences observed in the outcome of the Mitsunobu inversion of a secondary hydroxyl function attempted with both bicyclo[3.1.0]hexane nucleoside analogues could be explained by the rigid pseudoboat nature of this system. In one case, the bicyclic system facilitated formation of an anhydronucleoside intermediate, whereas in the other it completely prevented its formation. The chemically synthesized 5′-triphosphates of **1** and **2** were evaluated directly as RT inhibitors using both a recombinant enzyme and enzyme obtained and purified directly from wild-type viruses. The results showed that inhibition of RT occurred only with the conformationally locked $_2E$ (N)-*methano*-carba-AZT 5′-triphosphate. This inhibition was equipotent to and kinetically indistinguishable from that produced by AZT 5′-triphosphate. The antipodal $_3E$ (S)-*methano*-carba-AZT 5′-triphosphate, on the other hand, did not inhibit RT.

Introduction

AZT (3′-azido-3′-deoxythymidine) continues to play an important role in the therapy of treatment of AIDS, particularly in combination with other drugs. Drug combinations include other nucleoside analogues targeting the same enzyme, HIV reverse transcriptase (RT), non-nucleoside RT inhibitors, and more recently, protease inhibitors.[1] For this reason, a clearer understanding of the mechanism of action of AZT at the molecular level continues to be an important scientific and practical objective. Soon after the first successful clinical uses of AZT, nucleoside chemists attempted to correlate the conformational features of this drug to its biological properties with the intent of using this information as a paradigm for the development of other related antiretroviral nucleosides.[2] However, to date, a complete understanding of all the facets related to the mode of action of AZT, particularly those pertaining to the "active" conformation of the 5′-triphosphate anabolite responsible for efficient binding and inhibition of RT, has not been achieved.

The complete definition of the conformation of a nucleoside usually involves the determination of three principal structural parameters: (1) the glycosyl torsion angle χ (Figure 1A,B). which determines the syn or anti disposition of the base relative to the sugar moiety (syn when the C2 carbonyl of pyrimidines or N3 of purines lies over the sugar ring, anti when these atoms are oriented in the opposite direction); (2) the torsion angle γ (Figure 1C), which determines the orientation of the 5′-OH with respect to C3′ as represented by the three main rotamers, namely, $+sc$, ap, $-sc$; and (3) the puckering of the furanose ring and its deviation from planarity, which are described by the phase angle of pseudorotation P (0−360°, Figure 1D) and the maximum out-of-plane pucker ν_{max} ($\nu_{max} = \nu_2/\cos P$).[3] The value of P depends on the five endocyclic sugar torsion angles

† Laboratory of Medicinal Chemistry, Division of Basic Sciences, National Cancer Institute, National Institutes of Health.

‡ Experimental Retrovirology Section, Medicine Branch, Division of Clinical Sciences, National Cancer Institute, National Institutes of Health.

§ Laboratory for the Structure of Matter, Naval Research Laboratory.

(1) (a) For a recent review on the use of anti-HIV nucleosides, see: *Anti-HIV Nucleosides: Past, Present and Future*; Mitsuya, H., Ed.; R. G. Landes Co.: 810 S. Church St., Georgetown, TX, 1997. (b) Luzuriaga, K.; Bryson, Y.; Krogstad, P.; Robinson, J.; Stechenberg, B.; Lamson, M.; Cort, S.; Sullivan, J. L. *New Engl. J. Med.* **1997**, *336*, 1343. (c) Perelson, A. S.; Essunger, P.; Cao, Y.; Vesanen M.; Hurley, A.; Saksela, K.; Markowitz, M.; Ho, D. D. *Nature* **1997**, *387*, 188.

(2) (a) Van Roey, P.; Salerno, J. J.; Duax, W. L.; Chu, C. K.; Ahn, M. K.; Schinazi, R. F. *J. Am. Chem. Soc.* **1988**, *110*, 2277. (b) Van Roey, P.; Salerno, J. M.; Chu, C. K.; Schinazi, R. F. *Proc. Natl. Acad. Sci. U.S.A.* **1989**, *86*, 3929.

S0002-7863(97)03535-X
Published on Web 03/17/1998

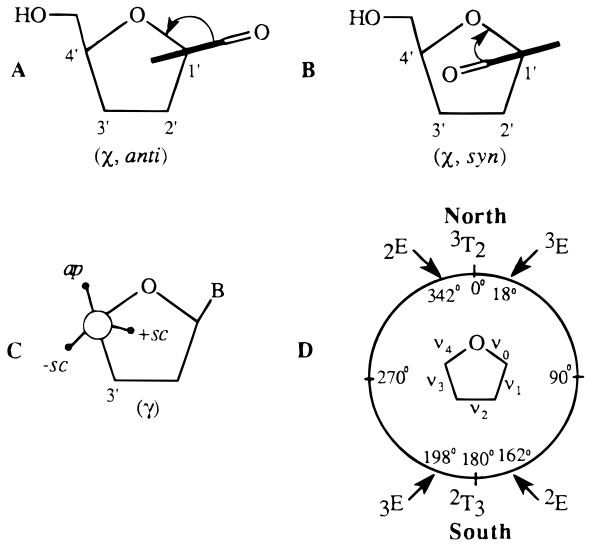

Figure 1. (A, B) Definition of anti and syn conformations for a pyrimidine nucleoside. χ is defined as torsion angle O4′−C1′−N1−C2. (C) Definition of the torsion angle ranges for γ about the C4′−C5′ bond. (D) Pseudorotational cycle of the furanose ring in nucleosides (E = envelope and T = twist).

ν_0−ν_4 (Figure 1D), and by convention, a phase angle $P = 0°$ corresponds to an absolute north conformation possessing a symmetrical twist form $^3T_2$, whereas its south antipode, $^2T_3$, is represented by $P = 180°$. The conformation of the furanose ring around the pseudorotational cycle alternates every 18° between envelope (E) and twist (T) conformations. Some of the most important envelope conformations discussed in this paper are highlighted in Figure 1D. The superscripts and subscripts represent, respectively, atoms displaced above or below the plane relative to other atoms in the five-membered ring. Atoms displaced on the same side as C5′ are called endo and those on the opposite side are called exo.

Any structure−activity relationship (SAR) study of anti-retroviral nucleosides is complicated by the complexity of the anabolic process of activation, which involves three sequential enzymatic steps to convert the nucleoside to its 5′-triphosphate (NTP), plus the final interaction of the NTP with the target enzyme, RT. Therefore, conformational preferences exhibited by the nucleoside, or its nucleotides, must be identified at each intervening enzymatic step. The only invariant step, common to all nucleoside RT inhibitors, is the final interaction of the NTP with RT. The route to the NTP anabolite, on the other hand, involves different cellular kinases all of which are highly dependent on the nature of the heterocyclic base.[1a]

In an earlier attempt to correlate anti-HIV activity with the conformational features of nucleosides, Van Roey et al. focused on the activation process and assumed that a similar conformation of the sugar moiety was required for all the steps leading to the NTP anabolite.[4] Hence, nucleoside analogues with a favorable 3′-exo ($_3E$) conformation, which is strongly associated with an *ap* torsion angle γ about the C4′−C5′ bond, were proposed to be the best substrates to generate abundant pools of the NTP anabolite. As a result, the plentiful amounts of NTP produced were expected to exhibit efficient inhibition of RT. This conformational analysis did not claim to include the critical RT binding step, however.[4,5] Hence, the correct interpretation of the overall biological response remained complicated by the fact that a very effective production of the NTP anabolite does not necessarily correlate with a higher binding affinity and potent inhibition of RT. In order to perform a more complete analysis, the two events—nucleoside activation and NTP interaction with RT—must be studied separately in terms of their conformational preferences. The main obstacle to this proposition is the inherent flexibility of the sugar ring, which equilibrates rapidly in solution between the two extreme forms of ring pucker: (i) the north conformation with P ranging between 342° and 18° ($_2E \rightarrow {}^3T_2 \rightarrow {}^3E$) and (ii) the opposite south conformation with values of P between 162° and 198° ($^2E \rightarrow {}^2T_3 \rightarrow {}_3E$). Preference for any of these specific conformations in solution is determined by the interplay of important interactions resulting from anomeric and gauche effects.[3b,6] In the solid state, however, only one of the two solution conformations is present, and its selection is additionally determined by crystal packing forces.[3b,7] Similarly, when a nucleoside or nucleotide binds to its target enzyme, only one form is expected to be present at the active site. Thus, any SAR study invoking the conformation of a nucleoside derived from an X-ray structure, or from a solution conformational analysis (i.e., NMR), is flawed since the binding conformation is likely to be altered by the enzyme to achieve optimal fitting. For this reason, we have conducted a definitive SAR study for the final RT binding step starting with conformationally locked nucleoside probes whose structural features in the solid state and in solution are virtually identical.

For the generation of such nucleoside analogues in which both solution and solid-state conformations are the same, we and others have used the bicyclo[3.1.0]hexane system as a convenient pseudosugar template.[8] This sugar surrogate exhibits a rigid pseudoboat conformation such that carbanucleosides constructed from it can adopt a fixed conformation that mimics the ring pucker of a true sugar moiety in a specific north or south conformation of the pseudorotational cycle. Because of the exclusive pseudoboat conformation of this template, a rigid north envelope $_2E$ conformation can be constructed when the cyclopropane ring is fused between C4′ and C6′. Conversely, fusion of the cyclopropane ring between C1′ and C6′ provides a rigid south $_3E$ envelope conformation. These changes are illustrated in Figure 2 for the two *methano*-carbocyclic isomers of AZT (**1** and **2**).[9] Since a specific form of ring pucker is known to be the strongest determinant in controlling the value

(3) (a) Altona, C.; Sundaranlingam, M. *J. Am. Chem. Soc*. **1972**, *94*, 8205. (b) For a comprehensive review of these concepts, see: Saenger, W. *Principles of Nucleic Acid Structure*; Springer-Verlag: New York, 1984.

(4) Van Roey, P.; Taylor, E. W.; Chu, C. K.; Schinazi, R. F. *Ann. N.Y. Acad. Sci.* **1990**, *616*, 29.

(5) Taylor, E. W.; Van Roey, P.; Schinazi, R. F.; Chu, C. K. *Antiviral Chem. Chemother*. **1990**, *1*, 163.

(6) Plavec, J.; Tong, W.; Chattopadhyaya, J. *J. Am. Chem. Soc.* **1993**, *115*, 9734.

(7) DeLeeuw, H. P. M.; Haasnoot, C. A. G.; Altona, C. *Isr. J. Chem.* **1980** *20*, 108.

(8) (a) Rodriguez, J. B.; Marquez, V. E.; Nicklaus, M. C.; Barchi, J. J., Jr. *Tetrahedron Lett.* **1993**, *34*, 6233. (b) Altmann, K.-H.; Kesselring, R.; Francotte, E.; Rihs, G. *Tetrahedron Lett.* **1994**, *35*, 2331. (c) Rodriguez, J. B.; Marquez, V. E.; Nicklaus, M. C.; Mitsuya, H.; Barchi, J. J., Jr. *J. Med. Chem.* **1994**, *37*, 3389. (d) Altmann, K.-H.; Imwinkelried, R.; Kesselring, R.; Rihs, G. *Tetrahedron Lett.* **1994**, *35*, 7625. (e) Ezzitouni, A.; Barchi, J. J., Jr.; Marquez, V. E. *J. Chem. Soc., Chem. Commun.* **1995**, 1345. (f) Jeong, L. S.; Marquez, V. E.; Yuan, C.-S.; Borchardt, R. T. *Heterocycles* **1995**, *41*, 2651. (g) Siddiqui, M. A.; Ford, H., Jr.; George, C.; Marquez, V. E. *Nucleosides Nucleotides* **1996**, *15*, 235. (h) Jeong, L. S.; Marquez, V. E. *Tetrahedron Lett.* **1996**, *37*, 2353. (i) Marquez, V. E.; Siddiqui, M. A.; Ezzitouni, A.; Russ, P.; Wang, J.; Wagner, R. W.; Matteucci, M. D. *J. Med. Chem.* **1996**, *39*, 3739. (j) Ezzitouni, A.; Marquez, V. E. *J. Chem. Soc., Perkin Trans. 1* **1997**, 1073. (k) Ezzitouni, A.; Russ, P.; Marquez, V. E. *J. Org. Chem.* **1997**, *62*, 4870.

(9) The correct numbering system for these compounds must follow the nomenclature for the bicyclo[3.1.0]hexane system. This numbering system is used in the Experimental Section and in the discussion of the chemical synthesis described in the text. However, a nucleoside numbering system, such as the one used in Figures 2 and 4, is utilized when comparing the conformation of these bicyclonucleosides with conventional nucleosides.

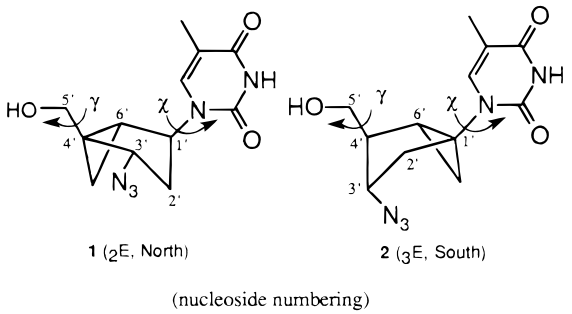

Figure 2. Conformationally locked forms of north and south *methano*-carba-AZT constructed on a bicyclo[3.1.0]hexane template.

of the other conformational parameters, namely χ and γ, one of the most valuable assets of these conformationally constrained nucleosides is their potential capacity to completely define the overall conformation of a nucleoside (or pseudonucleoside).[3b] The values of *P* and the torsion angles χ and γ are interdependent and change in a concerted manner to minimize steric clashes. For example, χ appears to prefer an anti disposition when the sugar presents a north ($_2E$) pucker, and the opposite syn disposition for a south ($_3E$) envelope.[3b] These preferences have been observed in the crystal structures of 8-bromoguanosine and 6-methyluridine, which, relative to the unsubstituted anti nucleosides, are forced to have χ in the syn range.[10] In both cases, the sugar pucker adjusts to the changes in χ by adopting a south ($_3E$) conformation.[3b]

For the present study, the two conformationally locked isomers of *methano*-carba-AZT (**1** and **2**) shown in Figure 2 were selected as synthetic targets. Compound **1** corresponds to a locked north ($_2E$) envelope conformation, and compound **2** corresponds to a locked south ($_3E$) envelope form. We shall describe the methods of synthesis used for these two compounds and highlight some distinctive chemical properties that are consistent with their established structures. The unique conformational preferences of **1** and **2** were corroborated by X-ray analysis, and solution NMR studies also confirmed the existence of equivalent and invariant pseudosugar pucker conformations for each individual isomer. The corresponding 5′-triphosphates of **1** and **2** were chemically synthesized and evaluated directly as inhibitors of RT using either a recombinant enzyme or the naturally occurring enzyme isolated from a mixture of wild-type HIV-1 strains. The results showed that inhibition of RT occurred almost exclusively with the conformationally locked north ($_2E$) *methano*-carba-AZT 5′-triphosphate, which was kinetically indistinguishable from the inhibition produced by AZT 5′-triphosphate. The antipodal rigid $_3E$ (south) conformer, on the other hand, did not inhibit RT. These results support an earlier NMR study that showed that AZT 5′-triphosphate and thymidine 5′-triphosphate bind to RT with a north conformation with χ in the anti range and γ as the $+sc$ rotamer.[11]

Chemical Synthesis

The two starting points for the synthesis of the azido compounds **1** and **2** were the corresponding *methano*-carbathymidine analogues, which have been previously reported.[8a,d,e,i−k] Thus, preparation of (N)-*methano*-carba-AZT (**1**) began with the partially protected (N)-*methano*-carbathymidine **3** (Scheme

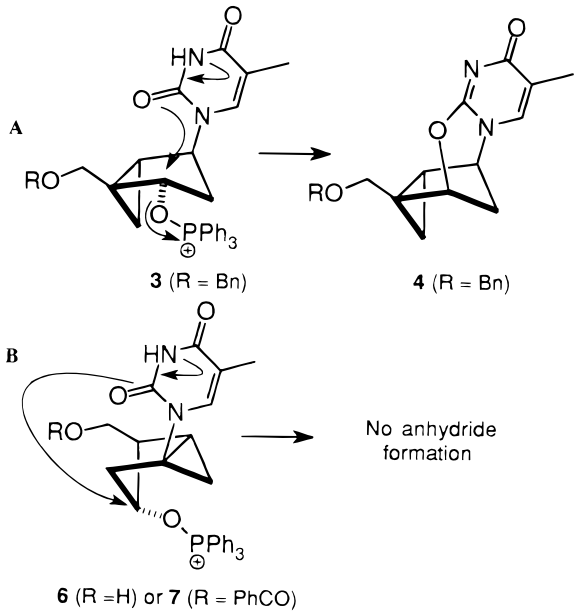

Figure 3. Reaction pathway of the Mitsunobu reaction on the north bicyclo[3.1.0]hexane template leading to anhydronucleoside **4** (A), and inability of the south bicyclo[3.3.0]hexane template to form an anhydronucleoside under the same reaction conditions (B).

Scheme 1

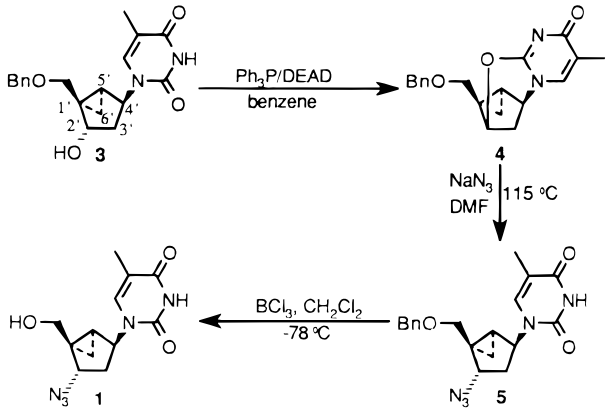

1). To introduce the azido group with the proper stereochemistry, an intermediary inversion at C2′ (carbocyclic numbering) was necessary.[9] Under Mitsunobu reaction conditions, formation of anhydronucleoside **4** was almost exclusive, thus rendering unnecessary the use of benzoic acid normally required by the reaction protocol to invert the stereochemistry of a secondary alcohol. In this situation, it is likely that the rigid pseudoboat conformation in **3** accelerates formation of the anhydronucleoside by facilitating intramolecular attack (Figure 3A). The resulting, very stable tetracyclic compound **4** underwent anhydride ring opening with azide at high temperature to give the corresponding protected (N)-*methano*-carba-AZT (**5**). Removal of the benzyl ether afforded the first target compound **1**.

The situation for the synthesis of (S)-*methano*-carba-AZT was less straightforward (Scheme 2). The same rigid bicyclo[3.1.0]-hexane system that facilitated anhydride formation from (N)-*methano*-carbathymidine (**3**) completely abrogated anhydride formation from (S)-*methano*-carbathymidine (**6**). This is shown schematically in Figure 3B, where it is evident that in the case of **6** the pyrimidine C2 oxygen cannot reach its target electrophilic carbon. Hence, standard Mitsunobu conditions were employed starting with unprotected (S)-*methano*-carbathymidine (**6**). The reaction proceeded with inversion of configuration at

(10) (a) Lai, T. F.; Marsh, R. E. *Acta Crystallogr. B* **1972**, *28*, 1982. (b) Green, E. A.; Rosenstein, R. D.; Shiono, R.; Abraham, D. J.; Trus, B. L.; Marsh, R. E. *Acta Crystallogr. B* **1975**, *31*, 102. (c) Tavale, S. S.; Sobell, H. M. *J. Mol. Biol.* **1970**, *48*, 109. (d) Suck, D.; Saenger, W. *J. Am. Chem. Soc.* **1972**, *94*, 6520.

(11) Painter, G. R.; Aulabaugh, A. E.; Andrews, C. W. *Biochem. Biophys. Res. Commun.* **1993**, *191*, 1166.

Scheme 2

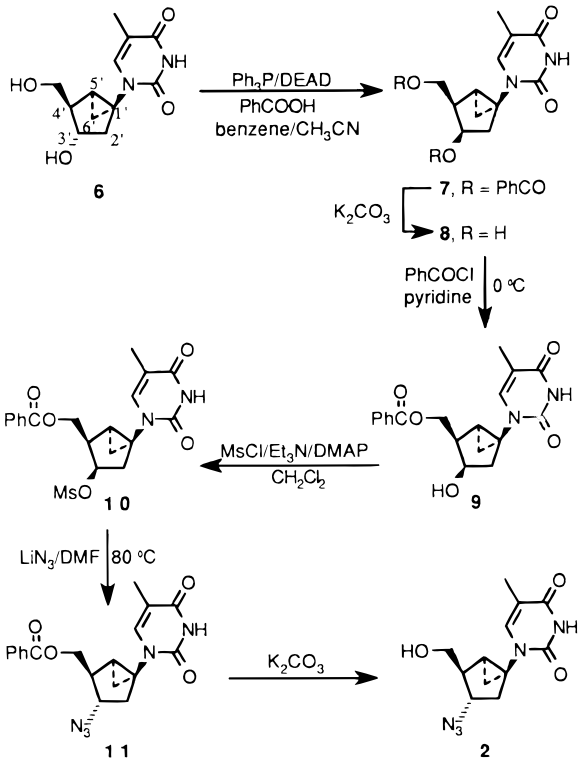

C3′ to give the corresponding dibenzoate ester **7**.[9] The contrast between the two Mitsunobu pathways followed by these reactions further validates the rigid pseudoboat conformation of the bicyclo[3.1.0]hexane system. The dibenzoate ester **7** was hydrolyzed to the corresponding diol **8**, which was then monoprotected as the monobenzoate ester **9**. Conversion of the secondary alcohol to the mesylate ester **10** was followed by nucleophilic displacement with azide to afford the corresponding protected (S)-*methano*-carba-AZT (**11**). Finally, base hydrolysis of the benzoate ester provided the second target compound **2**.

Synthesis of the corresponding 5′-triphosphates was performed using a "one-pot" approach by reacting nucleosides **1** and **2** with phosphorus oxychloride and subsequently treating the intermediates with tri-*n*-butylammonium pyrophosphate (see Experimental Section). The 5′-triphosphates of both **1** and **2** were obtained as sodium salts. Analytical HPLC showed that the predominant triphosphate peaks (area = 88.9−91.1%) eluted with retention times comparable to those of authentic AZT triphosphate (t_R = 33.2−34.0 min). The amount of diphosphate (t_R = 24.5−25 min) detected in both cases was ca. 5%.

X-ray Crystal Structures and Solid-State Conformational Analysis

The solid-state conformation of (N)-*methano*-carba-AZT (**1**) and (S)-*methano*-carba-AZT (**2**) agreed with the predictions outlined in Figure 2. The thermal ellipsoid plots are shown in Figure 4 and are labeled A for **1** and B and C for the two conformers of **2** that are present in the crystallographic asymmetric unit. Both structures show the expected pseudoboat conformation for the bicyclo[3.1.0]hexane system, which makes them reside, respectively, in nearly perfect $_2E$ and $_3E$ envelope conformations in the pseudorotational cycle (Figure 1, Table 1). The deviation of **1** from a perfect $_2E$ envelope is less than 2°, whereas the deviations of the two conformers of **2** from a perfect $_3E$ envelope are <1° and ca. 4°, respectively. In **1** the deviation of C2′ from the least-squares plane for atoms C1′, C3′, C4′, and C6′ (0.003 Å mean deviation from the plane) is 0.45 Å, which corresponds to a puckering amplitude of 29° (ν_{max}).[9] The corresponding mean deviation from the plane, atom deviation, and puckering amplitude in **2** for C3′ (molecule B) are 0.001 Å, 0.34 Å, and 22° (ν_{max}). For C13′ (molecule C) the corresponding values are 0.008 Å, 0.38 Å, and 24° (ν_{max}). Compared to the ribose puckering found in a large number of nucleosides (ν_{max} ca. 38.6°),[3b] the cyclopentane ring in a bicyclo-

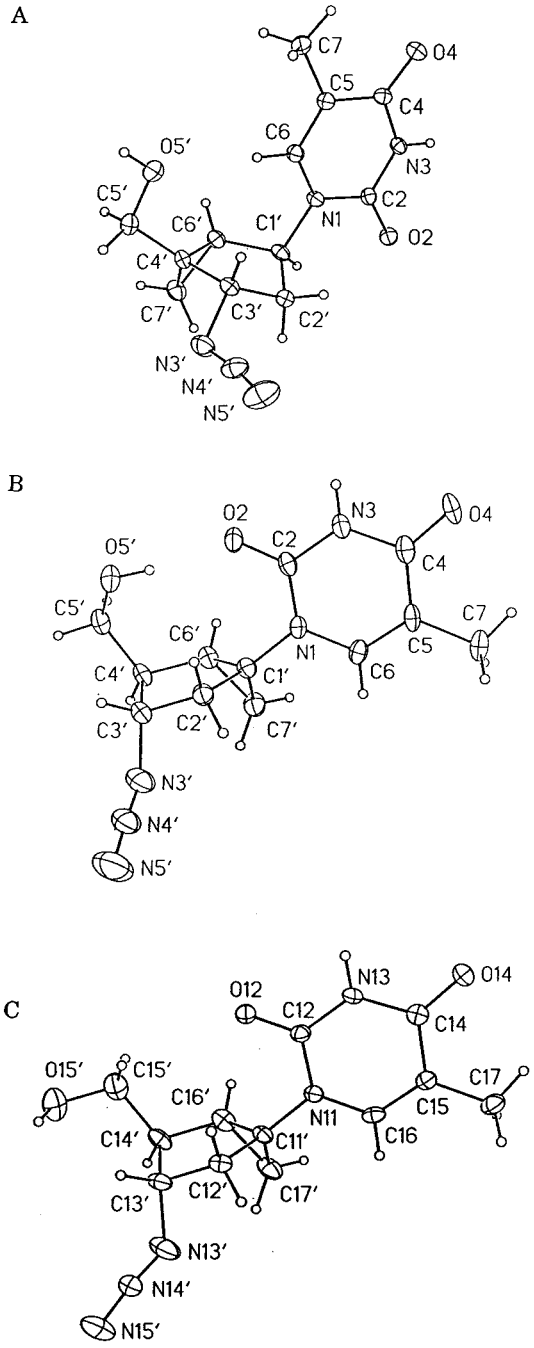

Figure 4. X-ray structures of (N)-*methano*-carba-AZT (**1**) (A) and two conformers of (S)-*methano*-carba-AZT (**2**) present in the crystallographic asymmetric unit (B, C).

Table 1. Conformational Parameters Calculated from X-ray Structures

compound	P (deg)	ν_{max} (deg)	χ (deg)	γ (deg)
1 (molecule A)	343.5	29	−147.3 (anti)	61.0 (+sc)
2 (molecule B)	197.8	22	62.5 (syn)	53.7 (+sc)
2 (molecule C)	193.7	24	66.5 (sym)	−73.6 (−sc)

[3.1.0]hexane system is somewhat flatter. The orientation of the ring substituents for **1** are pseudoequatorial for the azido and hydroxymethyl groups and pseudoaxial for the anti-oriented base, while, in both conformers of **2**, the syn-oriented base is disposed pseudoequatorially and the hydroxymethyl and azido groups are in a pseudoaxial disposition. The primary difference between the two conformers in **2** is the orientation of the hydroxymethyl group, which forms an intramolecular hydrogen bond involving the 5′-OH group and the O2 carbonyl group (molecule B, $\gamma = +sc$). In the second conformer (molecule C), the 15′-OH corresponds to a configuration where $\gamma = -sc$. In addition to the intramolecular hydrogen bond in **2**, there are three intermolecular hydrogen bonds; the imide hydrogen forms a hydrogen bond with a symmetry-related carbonyl O4, whereas in the second conformer the imide hydrogen binds to a symmetry-related carbonyl, O14. In the $-sc$ hydroxyl conformer, 15′-OH is a donor to O5′. In **1** the hydrogen bonds are intermolecular, involving the 5′-OH and the O2 carbonyl, and the imide hydrogen forms a hydrogen bond with the O4 carbonyl.

NMR Studies and Solution Conformational Analysis

We have previously used NMR spectroscopy to study the solution conformation of other north and south *methano*-carbanucleosides that contain the same fused bicyclo[3.1.0]-hexane system.[8a,c,e] The results from these studies were in accord with crystallographic data which unequivocally confirmed the exclusive pseudoboat pucker characteristic of this bicyclic system.[8b,d,g,i] Not surprisingly, both target compounds **1** and **2** showed the identical pseudoboat conformation as determined by X-ray crystallography (Figure 4), ^{1}H NMR coupling constants, and NOE analysis (vide infra). In the present investigation we have additionally attempted to ascertain the disposition of the glycosyl torsion angle χ in **1** and **2**, to determine if the exclusive preference for the anti and syn forms observed in their respective X-ray structures was also maintained in solution. For this purpose, we used one- (1D) and two-dimensional (2D) NOE experiments to qualitatively assess the range of conformational space sampled by the thymine base in both compounds. Other methods for estimating χ, such as measuring heteronuclear vicinal ^{13}C−^{1}H J coupling constants between the base and the glycone ring (i.e., $^3J_{H1'-C2}$) using a Karplus type equation,[12] are not as straightforward since the appropriate parameters for these bicyclic systems are lacking. Additionally, the south isomer **2** lacks a pseudoanomeric proton. In the following sections we describe the most salient features observed by NMR spectroscopy which corroborate the solid-state data and assist in the assignment of the syn/anti preferences observed for compounds **1** and **2**.

1. Coupling Constants and Chemical Shifts. From the X-ray structure in **1** (Figure 4A), the torsion angles H1′−C1′−C2′−H2′β and H1′−C1′−C6′−H6′ approach 90° (94.3° and 80.4°, respectively).[9] These values are analogous to those calculated previously for other conformationally locked north conformers using molecular modeling with the CHARMm force field.[8a] In close agreement with these values, the signal for H1′ in the ^{1}H NMR spectrum of **1** appeared as a doublet (δ 4.84, $^3J = 7.2$ Hz) coupled only to the signal at δ 1.75 belonging to H2′α.[9] Accordingly, the doublet of doublets at δ 2.10 was assigned to H2′β since it only couples to two protons (H2′α and H3′). In compound **2**, a notably small coupling constant was observed between H6′ and H4′, in agreement with the values of 84.7° and 85.8° measured for the dihedral angles H4′−C4′−C6′−H6′ and H14′−C14′−C16′−H16′ from structures B and C in Figure 4.[9] In addition, H2′α resonated as a clean doublet of $J = 13.5$ Hz, while H2′β was a doublet of a doublet of doublets (ddd) with J values of 2.3, 7.8, and 13.5 Hz. The small coupling of 2.3 Hz was assigned to a long-range interaction (*W*-type) with H7′$_{exo}$ which also appeared as a ddd containing a 2.3-Hz coupling constant. Long-range couplings of this type are relatively common in highly constrained systems.[13]

Particular proton chemical shifts and the differences in their values observed between compounds **1** and **2** were also diagnostic in our conformational assignment. For example, the difference in chemical shift ($\Delta\delta$) observed for H6 (thymine) between the two locked north and south isomers was 0.7 ppm (δ 7.83 for **1** and δ 7.13 for **2**). This suggests that in each molecule a significantly different magnetic environment is experienced by this proton, which is directly related to the disposition of the base in relation to the carbocyclic ring (χ angle, vide infra). The signals for H5′ and H5″ resonate within 0.2 ppm of one another in **2**, whereas the same signals appear separated by 1 ppm in compound **1**. From the large $\Delta\delta$ observed for the C5′ protons in **1**, it may be concluded that each proton experiences a separate environment which is relatively fixed with respect to the rest of the molecule, whereas for **2**, rotation about the C4′−C5′ bond is less encumbered.[9] Using the method of Haasnoot[14] to describe the γ rotamer population on the basis of the (H5′,H5″)−H4′ coupling constants is not possible for **1** and it could be ambiguous for **2** since the bicyclo[3.1.0]hexane system is quite different from a standard nucleoside. However, when this calculation is performed for compound **2** using the nucleoside convention for the stereospecific assignment of the 5′ protons (i.e., the *pro-R* proton is the signal resonating furthest downfield), the calculation predicts a 76% population of the $+sc$ rotamer. This agrees well with the disposition of γ found in one of the X-ray conformers of **2** (Figure 4B, Table 1). Analysis of the NOE spectra provided additional information for the stereospecific assignment of the C5′ protons (vide infra).

2. NOE Analysis. Both 1D and 2D NOE experiments were performed on compounds **1** and **2**. Steady-state 1D NOE difference spectra and 2D NOESY spectra provided data which allowed the determination of the preferred disposition of the base (χ angle) relative to the bicyclo[3.1.0]hexane ring in both cases. The data was collected in $CDCl_3$ with a small volume (5%) of CD_3OD to increase signal dispersion. The results of the NOESY spectra are summarized in Tables 2 and 3. It is clear from these experiments that the base prefers an anti disposition in compound **1** and a syn disposition in compound **2**. Figure 5 depicts the correlations associated with H6 in the 2D NOESY spectra of **1** and **2**. In compound **1**, H6 showed a strong correlation with H3′, as well as weaker interactions with H6′, H1′, H5′, and H5″. This stands in contrast to the data observed for **2** where H6 showed strong NOEs with H7′$_{exo}$ and H2′α, along with weaker correlations with H2′β and H7′$_{endo}$. No correlations were observed between H6 and H3′ or H5′,H5″, in either the steady-state (1D) or equilibrium (2D) NOE spectra of compound **2**. From the various NOE peaks observed, a qualitative measure of the preferred range of conformational space sampled by the thymine base (angle χ) can be estimated.

(12) (a) Plavec, J.; Koole, L. H.; Sandstrom, A.; Chattopadhyaya, J. *Tetrahedron* **1991**, *47*, 7363. (b) Lemieux, R. U.; Nagabhushan, T. L.; Paul, B. *Can. J. Chem.* **1972**, *50*, 773. (c) Davies, D. B. *Prog. Nucl. Magn. Reson. Spectrosc.* **1978**, *12*, 135.

(13) Rahman, A. *Nuclear Magnetic Resonance: Basic Principles*; Springer-Verlag: New York, 1986.

(14) Haasnoot, C. A. G.; de Leeuw, F. A. A. M.; Altona, C. *Tetrahedron* **1980**, *36*, 2783.

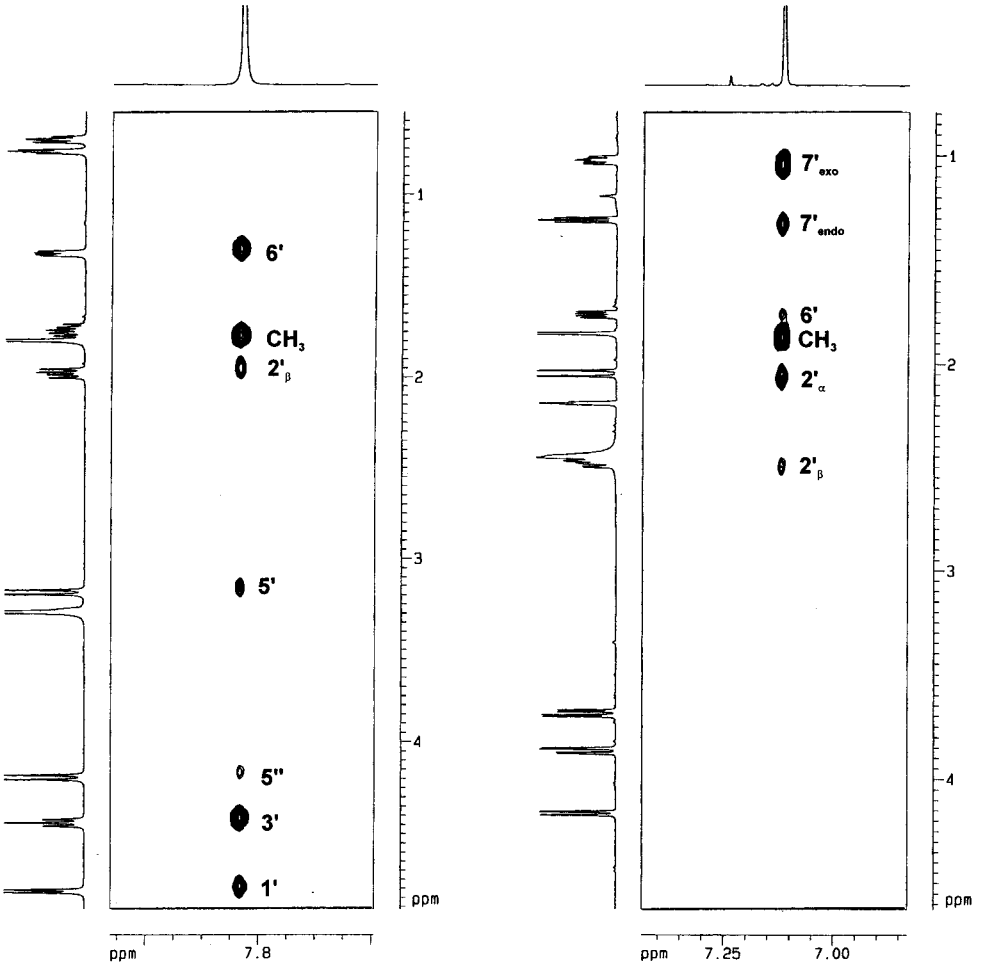

Figure 5. Section of the NOESY spectra of (N)-*methano*-carba-AZT (**1**) (A) and (S)-*methano*-carba-AZT (**2**) (B) showing the correlation between H6 on the thymine ring and other relevant signals of the bicyclo[3.1.0]hexane templates.

Table 2. NOESY Data for (N)-*methano*-Carba-AZT (**1**)

	cross-peak intensity[a]										
								H7′			
	H1′	H2′α	H2′β	H3′	H5′	H5″	H6′	exo	endo	H6	CH_3
H1′		s	m				m		m	m	
H2′α	s		s	w					s		
H2′β	m	s		s						w	
H3′		w	s			w				s	
H5′						s		w		vw	
H5″					s		m	s		w	
H6′	m					m		m	w	m	
H7′											
exo					w	s	m		m		
endo	m	s					vw	m			
H6	m		w	s	vw	w	m				s
CH_3										s	

[a] Cross-peak intensities are divided into four groups: strong (s), medium (m), weak (w), and very weak (vw).

Table 3. NOESY Data for (S)-*methano*-Carba-AZT (**2**)

	cross-peak intensity[a]										
								H7′			
	H2′α	H2′β	H3′	H4′	H5′	H5″	H6′	exo	endo	H6	CH_3
H2′α		s	m						m	m	
H2′β	s		s		w	vw				vw	
H3′	m	s		m	w	m					
H4′			m		m	w	m	w	m		
H5′		m	w	m		s	m				
H5″		vw	m	m	s		w				
H6′				m	m	w		s		vw	
H7′											
exo				w			s		s	s	
endo	m			m				s		w	
H6	m	w					vw	s	w		s
CH_3										s	

[a] Cross-peak intensities are divided into four groups: strong (s), medium (m), weak (w), and very weak (vw).

The resulting ranges of χ proposed for compounds **1** and **2** are shown in Figure 6. These ranges were assessed by comparing the intensities of the NOEs in both the 1D and 2D datasets and setting qualitative limits on the positioning of the H6 proton by the absence of a correlation on other relevant protons. The convention similar to that used for standard O4′-containing nucleosides was used,[3b] where χ is defined by atoms C6′−C1′−N1−C2.[9] An anti distribution typically observed for $_2E$ (or 3′-endo) nucleosides favoring a range of χ between −90° and 170° could be predicted for **1**, whereas in **2** a more constrained syn range between 0° and 50° was presumed from the data (Figure 6). These results agree with the preferred dispositions observed for the base in the X-ray crystal structures. In addition, the different disposition of the thymine ring offers an explanation for the large difference in chemical shift observed for the H6 proton in compounds **1** and **2**. The syn relation of the base to the carbocyclic ring in **2** would orient H6 toward the concave endo face of the bicyclic ring system, resulting in the shielding of this proton from the orbitals of the carbon framework.[13]

The distribution of γ determined from the coupling constant data discussed above was determined only for compound **2** since compound **1** does not contain a C4′ proton. From the NOE

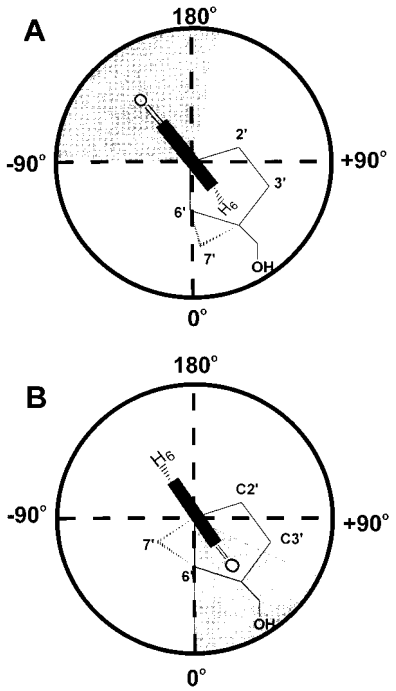

Figure 6. Restricted values of χ in the anti and syn domains for the thymine base in (N)-*methano*-carba-AZT (**1**) (A) and (S)-*methano*-carba-AZT (**2**) (B) as inferred from NOE experiments.

data in compound **2** it could be concluded that both $+sc$ and *ap* conformations are populated as inferred from the correlations observed for H5′ and H5″. For compound **1**, however, the NOE data predicts the predominance of the $+sc$ rotamer due to the stronger interactions of H5″ with both H6′ and H7′$_{exo}$, plus the lack of significant correlation for the H5′ proton with any resonance other than H5″.

According to the discussion above, a broader range of conformational space is sampled by the thymine base in compound **1** and, correspondingly, by the hydroxymethyl group of compound **2**. These observations imply that the appendages which form the quaternary centers at the bridgehead of this bicyclic system (i.e., the base in **2** and the CH_2OH in **1**) are more rotationally restricted than when these groups are simply extended from the five-membered ring (i.e., the base in **1** and the CH_2OH in **2**). From these studies we conclude that the fused cyclopropyl ring serves to influence the flexibility of the relevant structural parameters available to these unique analogues. Hence, on the basis of the demonstrated virtual equivalence of solid-state and solution conformations in each case, we can surmise that the conformations with which these compounds encounter the enzyme(s) are essentially invariant.

Inhibition of Reverse Transcriptase

Reverse transcription by RT represents an essential step for retroviral replication. In this critical step, substrate binding is ordered: nucleic acid template-primer binding is followed by the high-affinity binding of the correct 2′-deoxynucleoside 5′-triphosphate complementary to the next position on the template.[15] Incorporation of the new nucleotide unit into the nascent chain then occurs via S_N2 displacement of the pyrophosphate by the 3′-hydroxyl of the preceding nucleotide unit. Misincorporation of a modified nucleotide lacking the 3′-hydroxyl moiety, such as AZT 5′-triphosphate, results in premature chain termination and inhibition of the polymerase function of RT. When a deoxy mimic of the RNA template was used as a nucleic acid template-primer, and cocrystallized with HIV-1 RT, it showed the DNA significantly bent in an area where the template-primer contacts the αH of the p66 thumb.[16] Prior to this bend, near the polymerase active site, the template resembles canonical A-form DNA, whereas the template-primer resembles B-form DNA in the region between the bend and the RNAase H domain.[16] It is not too surprising, therefore, that the polymerase domain of RT should bind to the incoming 5′-triphosphates preferentially with a north sugar conformation characteristic of A-form DNA. This preference was recently suggested by the work of Painter et al., who also showed that the orientation of the glycosyl angle χ for AZT 5′-triphosphate bound to RT was in the anti range, and that the preferred torsion angle γ was in the $+sc$ range.[11] Since these conformational restrictions are met by the (N)-*methano*-carba-AZT 5′-triphosphate, this compound represents an excellent probe to test conclusively RT's preference for a north, A-form DNA conformation for the incoming 5′-triphosphate. Conversely, the (S)-*methano*-carba-AZT 5′-triphosphate would present the enzyme with the antipodal south conformation in which the glycosyl torsion angle χ is additionally restricted to the syn range. On the basis of these premises, we predicted that RT would bind preferentially to (N)-*methano*-carba-AZT 5′-triphosphate. What was impossible to predict beforehand, however, was whether this conformationally rigid 5′-triphosphate would bind as well as the more malleable AZT 5′-triphosphate. The results showed that the potency and kinetics of RT inhibition by (N)-*methano*-carba-AZT 5′-triphosphate was indistinguishable from that produced by AZT 5′-triphosphate (Figure 7). On the other hand, (S)-*methano*-carba-AZT 5′-triphosphate failed to significantly inhibit the enzyme. The selective inhibition of RT shown by (N)-*methano*-carba-AZT 5′-triphosphate was similar for a recombinant enzyme (Figure 7A), as well as for an enzyme obtained from a mixture of HIV-1 strains (HIV-1_{LAI}, Figure 7B).

Final Remarks and Conclusions

The underlying concept for the synthesis of carbocyclic nucleosides (carbanucleosides) was the generation of a stable C−N bond resistant to chemical and enzymatic hydrolysis, while at the same time causing minimal structural changes.[17] However, the absence of the 4′-oxygen represents a dramatic change in terms of stereoelectronic effects, and the structural changes ensuing its removal are quite significant. In carbanucleosides, the anomeric effect, as well as important gauche interactions between the 4′-oxygen and any electronegative substituents (e.g., OH, N_3, F, etc.) occupying positions C2′ and C3′, is abolished. Normally, the combined effect of these important interactions drives the conformation of the sugar ring of conventional nucleosides into a preferred north or south hemisphere. In solution, the conformation of a nucleoside is represented by an equilibrium between these two extremes, and the direction of

(15) (a) Majumdar, C.; Abbotts, J.; Broder, S.; Wilson, S. H. *J. Biol. Chem.* **1988**, *263*, 15657. (b) Kedar, P. S.; Abbotts, J.; Kovacs, T.; Lesiak, K.; Torrence, P.; Wilson, S. H. *Biochemistry* **1990**, *29*, 3603. (c) Reardon, J. E.; Miller, W. H. *J. Biol. Chem.* **1990**, *265*, 20302. (d) Kati, W. M.; Johnson, K. A.; Jerva, L. F.; Anderson, K. S. *J. Biol. Chem.* **1992**, *267*, 25988. (e) Hsie, J.: Zinnen, S.; Modrich, P. *J. Biol. Chem.* **1993**, *268*, 24607. (f) Rittinger, K.; Divita, G.; Goody, R. S. *Proc. Natl. Acad. Sci. U.S.A.* **1995**, *92*, 8046.

(16) Jacobo-Molina, A.; Ding, J. P.; Nanni, R. G.; Clark, A. D.; Lu, X. D.; Tantillo, C.; Williams, R. L.; Kamer, G.; Ferris, A. L.; Clark, P.; Hizi, A.; Hughes, S. H.; Arnold, E. *Proc. Natl. Acad. Sci. U.S.A.* **1993**, *90*, 6320.

(17) (a) Marquez, V. E.; Lim, M.-I. *Med. Res. Rev.* **1986**, *6*, 1. (b) Borthwick, A. D.; Biggadike, K. *Tetrahedron* **1992**, *48*, 571. (c) Agrofoglio, L.; Suhas, E.; Farese, A.; Condom, R.; Challand, S. R.; Earl, R. A.; Guedj, R. *Tetrahedron* **1994**, *50*, 10611. (d) Marquez, V. E. Carbocyclic nucleosides. In *Advances in Antiviral Drug Design*; De Clercq, E., Ed.; JAI Press Inc.: Greenwich, CT, 1996; Vol. 2, pp 89−146.

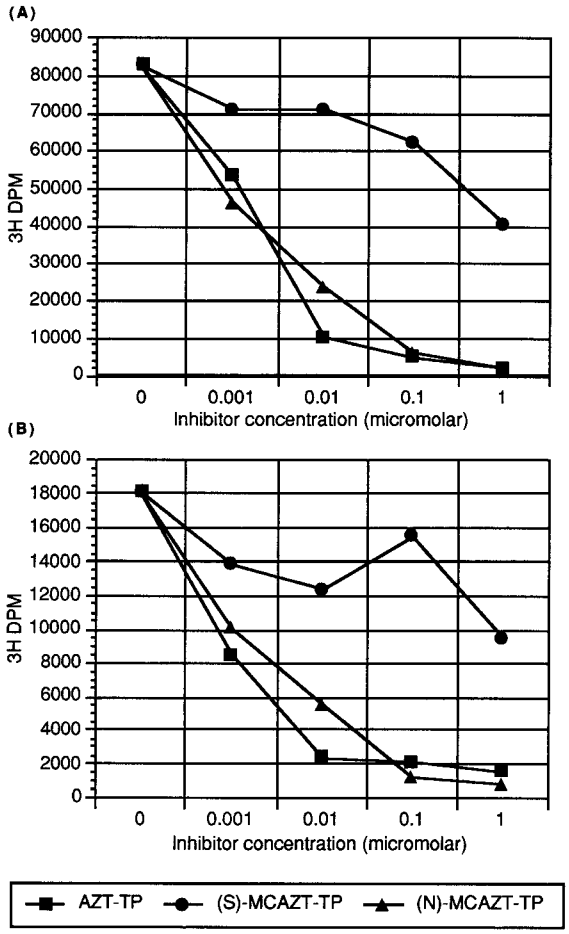

Figure 7. Inhibition of RT by (N)-*methano*-carba-AZT 5′-triphosphate (▲), AZT 5′-triphosphate (■), and (S)-*methano*-carba-AZT 5′-triphosphate (●) from a recombinant enzyme from a wild-type virus (RT_{BH10}) (A) and naturally occurring enzyme purified from a mixture of HIV-1 ($HIV\text{-}1_{LAI}$) strains (B). Results are expressed as DPM of [^{3}H]TMP incorporated.

this equilibrium is often determined by the interplay of the above-mentioned forces. In the solid state, however, generally only one of the two typical solution conformations is present. Similarly, when a nucleoside or nucleotide binds to its target enzyme, only one form is present in the drug−receptor complex. Since the cyclopentane ring in conventional carbanucleosides exists in an unusual 1′-exo form (as in carbathymidine and carba-AZT),[18] we have constructed a new class of *methano*-carbanucleosides using a bicyclo[3.1.0]hexane template which produces conformationally locked forms of ring pucker that mimic the $_2E$ (north) and $_3E$ (south) conformations of conventional nucleosides (Figure 2). It has been suggested that AZT's preference in the crystal structure for an extreme $_3E$ (south) conformation is responsible for its potent anti-HIV activity.[2,4] On the other hand, there is evidence that AZT 5′-triphosphate binds to RT in a north conformation.[11] To resolve this issue we constructed conformationally locked $_2E$ and $_3E$ carba-AZT 5′-triphosphates and tested their ability to inhibit RT using both a recombinant enzyme and a wild-type enzyme isolated from several HIV-1 strains. In both cases it was found that enzyme inhibition occurred exclusively with the north *methano*-carba-AZT 5′-triphosphate. The IC_{50} of ca. 1 nM was equal to that of AZT 5′-triphosphate, used as a reference in the same experiment. We were also able to confirm by X-ray analysis that the designed structures of the parent *methano*-carbanucleosides conformed to the designed features of the bicyclo[3.1.0]-hexane system, and that the resulting templates provided conformationally locked north (N)-*methano*-carba-AZT (**1**) and south (S)-*methano*-carba-AZT (**2**). Through the use of NMR analysis we also established that the solution conformations of **1** and **2** were virtually identical to their corresponding solid-state conformations. This virtual equivalence of solution and solid-state conformations allowed us to probe the conformational preference of AZT 5′-triphosphate bound to RT. While these results determine what that conformational preference is, it does not appropriately answer the question of activation, since neither carbocyclic AZT analogue **1** or **2** showed anti-HIV activity per se against infected ATH8 cells in vitro (unpublished results). Recalling the hypothesis[2,4] that a preferred south ($_3E$) conformation is required for efficient interaction with the kinase(s), one can explain why (N)-*methano*-carba-AZT (**1**), which is permanently locked in an antipodal north ($_2E$) conformation, is not efficiently phosphorylated. On the other hand, the chances for the south (S)-*methano*-carba-AZT (**2**), which has the required south ($_3E$) conformation for efficient phosphorylation, appear to be compromised by the unexpected rigidity of the torsion angle χ which forces the orientation of the thymine base into a permanent syn orientation. Using these arguments one can understand why flexible nucleosides function better as prodrugs of the biologically active nucleotides. For example, AZT by its flexible nature can adopt a south ($_3E$) conformation required for phosphorylation and subsequently switch to a north ($_2E$) conformation for a better interaction with RT. Indeed, solution conformation studies by NMR have confirmed that the north and south pseudorotamer populations of the furanose ring of AZT are approximately equal,[12a] while Raman spectroscopy suggests that the north conformer is somewhat predominant.[19] This capacity to adopt different forms of ring pucker is a characteristic of natural nucleosides, and it is perhaps the reason why nature selected ribofuranoses and not the more rigid ribopyranoses as the building blocks of nucleic acids.[20] In ribofuranosides, different factors such as gauche effect and anomeric effect, and their influence on pseudorotation, could explain the enormous disparity in anti-HIV activity that is evident for a large number of 2′,3′-dideoxynucleosides, despite their apparent structural similarity. Biochemically, this divergence could result from differences in the ability of the individual dideoxynucleosides to adopt with ease both required north and south conformations. We propose that the use of conformationally restricted analogues of nucleosides can also help discern the specific preference of the various kinases involved in the activation of nucleosides. In addition, the use of various prodrug approaches to overcome the lack of phosphorylation might be of practical use to increase specificity and reduce toxicity arising from the accumulation of unwanted intermediate anabolites. Pro-nucleotide drug studies are currently under investigation with (N)-*methano*-carba-AZT (**1**).

Experimental Section

General Procedures. All chemical reagents were commercially available. Melting points were determined on a Fisher-Johns melting point apparatus and are uncorrected. Column chromatography was

(18) (a) Kalman, A.; Koritsanzky, T.; Beres, J.; Sagi, G. *Nucleosides Nucleotides* **1990**, *9*, 235. (b) Bodenteich, M.; Griengl, H. *Tetrahedron Lett.* **1987**, *28*, 5311.

(19) Dijkstra, S.; Benevides, J. M.; Thomas, G. J., Jr. *J. Mol. Struct.* **1991**, *242*, 283.

(20) (a) Eschenmoser, A.; Dobler, M. *Helv. Chim. Acta* **1992**, *75*, 218. (b) Pitsch, S.; Wendeborn, S.; Jaun, B.; Eschenmoser, A. *Helv. Chim. Acta* **1993**, *76*, 2161. (c) Otting, G. Billeter, M.; Wuthrich, K.; Roth, H. J.; Leumann, C.; Eschenmoser, A. *Helv. Chim. Acta* **1993**, *76*, 2701. (d) Schlonvogt, I.; Pitsch, S.; Lesueur, C.; Eschenmoser, A.; Jaun, B.; Wolf, R. M. *Helv. Chim. Acta* **1996**, *79*, 2316.

performed on silica gel 60, 230−400 mesh (E. Merck), and analytical TLC was performed on Analtech Uniplates silica gel GF. Routine IR and ^{1}H and ^{13}C NMR spectra were recorded using standard methods. Specific rotations were measured in a Perkin-Elmer model 241 polarimeter. Positive-ion fast-atom-bombardment mass spectra (FABMS) were obtained on a VG 7070E mass spectrometer at an accelerating voltage of 6 kV and a resolution of 2000. Glycerol was used as the sample matrix, and ionization was effected by a beam of xenon atoms. Elemental analyses were performed by Atlantic Microlab, Inc., Norcross, GA.

(1′*R*,2′*R*,4′*S*,5′*S*)-1′-[(Benzyloxy)methyl]-2,2′-anhydro-4′-(5-methyl-4-(1*H*)-oxopyrimidin-1-yl)bicyclo[3.1.0]hexane (4). A mixture of **3** (0.250 g, 0.73 mmol) and triphenylphosphine (0.38 g, 1.46 mmol) was stirred in dry benzene (25 mL) and treated with diethyl azodicarboxylate (DEAD, 0.23 mL, 1.46 mmol). The reaction mixture was stirred further at ambient temperature for 2 h under argon, after which time the solvent was removed under reduced pressure. The crude residue was purified by flash column chromatography (silica gel, gradient 0 → 10% MeOH/CH_2Cl_2) to give **4** (0.173 g, 73%) as a solid: mp 158−160 °C; ^{1}H NMR ($CDCl_3$) δ 7.40−720 (m, 5 H, Ph), 6.85 (s, 1 H, H-6), 5.07 (br s, 1 H, H-4′), 4.50 (AB q, J = 11.9 Hz, 2 H, $PhCH_2O$), 4.15 (m, 2 H, H-2′, $PhCH_2OCHH$), 3.10 (d, J = 10.0 Hz, 1 H, $PhCH_2OCHH$), 2.15−1.90 (m, 5 H, H-3′$_{a,b}$, CH_3), 1.78 (t, J = 5.5 Hz, 1 H, H-5′), 0.87 (d, J = 5.6 Hz, 2 H, H-6′$_{a,b}$); FABMS *m*/*z* (relative intensity) 325 (MH^+, 40), 217 ($MH^+ - PhCH_2OH$, 8), 91 ($PhCH_2^+$, 100). This compound was used in the next step without further purification.

(1′*S*,2′*S*,4′*S*,5′*S*)-1′-[(Benzyloxy)methyl]-2′-azido-4′-(5-methyl-2,4-(1*H*,3*H*)-dioxopyrimidin-1-yl)bicyclo[3.1.0]hexane (5). A solution of anhydride **4** (0.090 g, 0.27 mmol) in DMF (30 mL) was treated with sodium azide (0.36 g, 5.53 mmol) and heated at 120 °C (oil bath) for 96 h. The reaction mixture was allowed to cool to ambient temperature, treated with water (40 mL), and extracted with EtOAc (3 × 75 mL). The combined organic extract was washed with brine (100 mL), dried ($MgSO_4$), and reduced to dryness. The crude residue was purified by flash column chromatography (silica gel, gradient 0 → 75% EtOAc/hexane) to give **5** (0.061 g, 60.3%) as a thick oil, which solidified to an amorphous solid after cooling to 4 °C: ^{1}H NMR ($CDCl_3$) δ 8.40 (br s, 1 H, NH), 7.80 (s, 1 H, H-6), 7.40−720 (m, 5 H, Ph), 5.00 (d, J = 6.9 Hz, 1 H, H-4′), 4.55 (AB q, J = 11.4 Hz, 2 H, $PhCH_2O$), 4.50 (t, J = 9.3 Hz, 1 H, H-2′), 4.15 (d, J = 10.3 Hz, 1 H, $PhCH_2OCHH$), 3.18 (d, J = 10.3 Hz, 1 H, $PhCH_2OCHH$), 2.00 (dd, J = 15.2, 8.5 Hz, 1 H, H-3′$_a$), 1.80 (m, 1 H, H-3′$_b$), 1.50 (s, 3 H, CH_3), 1.38 (dd, J = 8.5, 3.9 Hz, 1 H, H-5′), 0.90−0.70 (m, 2 H, H-6′$_{a,b}$). Anal. Calcd for $C_{19}H_{21}N_5O_3$: C, 62.11; H, 5.76; N, 19.06. Found: C, 61.98; H, 5.85; N, 18.77.

(1′*S*,2′*S*,4′*S*,5′*S*)-1′-(Hydroxymethyl)-2′-azido-4′-(5-methyl-2,4-(1*H*,3*H*)-dioxopyrimidin-1-yl)bicyclo[3.1.0]hexane (1). Under an atmosphere of argon, a stirred solution of **5** (0.037 g, 0.101 mmol) in anhydrous CH_2Cl_2 (15 mL) was cooled to −78 °C and treated with a solution of BCl_3 (1.4 mL, 1 M solution in CH_2Cl_2). After 4 h, the reaction was quenched with MeOH (2 mL) and the mixture allowed to warm to ambient temperature and then concentrated under reduced pressure. The residue was coevaporated with MeOH (3 × 10 mL), and the crude product was purified, first by flash column chromatography (silica gel, gradient 50 → 80% EtOAc/hexane) and then by recrystallization from $CHCl_3$/hexane to give 0.023 g (82%) of **3** as a white crystalline material: mp 173−4 °C; IR (KBr) 2100 cm^{-1}; $[\alpha]_D$ = +12 (*c* 0.9; MeOH); ^{1}H NMR ($CDCl_3$) δ 9.65 (s, 1 H, NH), 7.83 (s, 1 H, H-6), 4.84 (d, J = 7.2 Hz, 1 H, H-4′), 4.60 (t, J = 8.9 Hz, 1 H, H-2′), 4.33 (d, J = 11.5 Hz, 1 H, C*H*HOH), 3.33 (d, J = 11.5 Hz, 1 H, CH*H*OH), 2.10 (dd, J = 15.1, 8.6 Hz, 1 H, H-3′$_a$), 1.95−1.78 (m, 1 H, H-3′$_b$), 1.85 (s, 3 H, CH_3), 1.50 (dd, J = 8.3, 4.0 Hz, 1 H, H-5′), 0.88−0.75 (m, 2 H, H-6′$_{a,b}$); ^{13}C NMR ^{1}H NMR ($CDCl_3$) δ 10.71, 12.38, 25.98, 36.14, 36.19, 57.31, 60.43, 63.52, 110.90, 138.13, 151.17, 164.06; FABMS *m*/*z* (relative intensity) 278 (MH^+, 100), 127 (Thy + 2H, 57). Anal. Calcd for $C_{12}H_{15}N_5O_3 \cdot 1.25H_2O$: C, 48.07; H, 5.88; N, 23.36. Found: C, 48.20; H, 5.71; N, 23.26.

(1′*S*,3′*R*,4′*R*,5′*S*)-3′-(Benzoyloxy)-4′-[(benzoyloxy)methyl]-1′-(5-methyl-2,4-(1*H*,3*H*)-dioxopyrimidin-1-yl)bicyclo[3.1.0]hexane (7). Under an atmosphere of argon, a solution of compound **6** (0.55 g, 2.18 mmol), triphenylphosphine (2.29 g, 8.72 mmol), and benzoic acid (1.065 g, 8.72 mmol) in a mixture of benzene/acetonitrile (40/8 mL) was stirred at 0 °C. Diethyl azodicarboxylate (DEAD, 1.37 mL, 8.72 mmol) was added dropwise during the course of 10 min, the ice bath was removed, and stirring was continued at room temperature for 12 h. The solvent was evaporated to dryness and the residue was purified by flash chromatography (silica gel, Et_2O/hexane, 9/1) to provide a white solid still contaminated with Ph_3P. A second chromatography was required to yield **7** (1.0 g, 99.6%) as a white foam: mp 174−176 °C; ^{1}H NMR ($CDCl_3$) δ 9.01 (d, J < 1 Hz, 1 H, NH), 7.95−7.85 and 7.55−7.28 (m, 10 H, Ph), 7.14 (s, 1 H, H-6), 5.15 (dd, J = 16.6, 7.6 Hz, 1 H, H-3′), 4.71 (d, J = 6.2 Hz, 2 H, $PhCOOCH_2$), 2.97 (dd, J = 13.4, 6.4 Hz, 1 H, H-4′), 2.75 (dd, J = 12.3, 7.6 Hz, H-2′$_a$), 2.50 (dd, J = 12.1, 9.5 Hz, 1 H, H-2′$_b$), 1.92 (dd, J = 8.5, 5.9 Hz, 1 H, H-5′), 1.72 (d, J < 1 Hz, 3 H, CH_3), 1.22−1.10 (m, 2H, H-6′$_{a,b}$). Anal. Calcd for $C_{26}H_{24}N_2O_6$: C, 67.82; H, 5.25; N, 6.08. Found: C, 67.70; H, 5.30; N, 5.98.

(1′*S*,3′*R*,4′*R*,5′*S*)-3′-Hydroxy-4′-(hydroxymethyl)-1′-(5-methyl-2,4-(1*H*,3*H*)-dioxopyrimidin-1-yl)bicyclo[3.1.0]hexane (8). A stirred solution of **7** (1.00 g, 2.172 mmol) in MeOH (30 mL) was treated with K_2CO_3 (0.45 g, 2.172 mmol) overnight at ambient temperature. The solvent was evaporated to dryness and the residue was purified by flash column chromatography (silica gel, first EtOAc, followed by $CHCl_3$/MeOH, 9/1) to give **8** (0.40 g, 73%) as a white solid: mp 123−125 °C; ^{1}H NMR ($CDCl_3$) δ 7.12 (d, J < 1 Hz, 1 H, H-6), 5.04−3.95 (m, 3 H, CH_2OH, H-3′), 2.47 (dd, J = 12.3, 7.6 Hz, 1 H, H-2′$_a$), 2.24 (m, 1 H, H-4′), 2.12 (ddd, J = 12.0, 8.1, 1.3 Hz, 1 H, H-2′$_b$), 1.89 (d, J < 1 Hz, 3 H, CH_3), 1.80 (dd, J = 9.6, 4.8 Hz, 1 H, H-5′), 1.00 (m, 1 H, H-6′$_a$), 0.81 (irregular t, J ca. 5.3 Hz, 1H, H-6′$_b$). Anal. Calcd for $C_{12}H_{16}N_2O_4$: C, 56.13; H, 6.47; N, 10.91. Found: C, 56.33; H, 6.33; N, 10.57.

(1′*S*,3′*R*,4′*R*,5′*S*)-3′-Hydroxy-4′-[(benzoyloxy)methyl]-1′-(5-methyl-2,4-(1*H*,3*H*)-dioxopyrimidin-1-yl)bicyclo[3.1.0]hexane (9). A stirred solution of **8** (0.35 g, 1.387 mmol) in anhydrous pyridine (15 mL) was cooled to 0 °C and treated with benzoyl chloride (194 μL, 1.665 mmol). After 2 h at 0 °C, the ice bath was removed, and stirring was continued at ambient temperature for 12 h. The temperature was lowered again to 0 °C, and additional benzoyl chloride (81 μL, 0.7 mmol) was added. After 2 h of stirring at ambient temperature the solvent evaporated to dryness, and traces of pyridine were removed by coevaporation with toluene (3 × 10 mL). The residue was purified by flash column chromatography (silica gel, first with EtOAc, followed by 5% MeOH/CH_2Cl_2) to give **9** (0.37 g, 74.3%) as a white solid: mp 94−96 °C; NMR ($CDCl_3$) δ 9.30 (br s, 1 H, NH), 8.10−7.96 and 7.55−7.35 (m, 5 H, Ph), 7.12 (s, 1 H, H-6), 4.70 (m, 2 H, $PhCOOCH_2$), 4.20 (dd, J = 10.3, 5.2 Hz, 1 H, H-3′), 2.45−2.25 (m, 2 H, H-4′, H-2′$_a$), 2.11 (dd, J = 13.7, 3.4 Hz, 1 H, H-2′$_b$), 1.85 (ddd, J = 9.6, 4.6, 1.5 Hz, 1 H, H-5′), 1.78 (s, 3 H, CH_3), 1.32 (dd, J = 9.5, 6.3 Hz, 1 H, H-6′$_a$), 1.00 (irregular t, J ca. 5.3 Hz, H-6′$_b$). Anal. Calcd for $C_{19}H_{20}N_2O_5 \cdot 1.15$ CH_2Cl_2: C, 53.28; H, 4.91; N, 6.16. Found: C, 53.29; H, 4.98; N, 6.14.

(1′*S*,3′*S*,4′*S*,5′*S*)-3′-Azido-4′-[(benzoyloxy)methyl]-1′-(5-methyl-2,4-(1*H*,3*H*)-dioxopyrimidin-1-yl)bicyclo[3.1.0]hexane (11). A stirred solution of **9** (0.35 g, 0.982 mmol) in CH_2Cl_2 (20 mL) containing triethylamine (0.684 mL) and (dimethylamino)pyridine (0.012 g) was cooled to 0 °C and treated slowly with methanesulfonyl chloride (0.191 mL, 1.964 mmol). After 2 h, the solvent was evaporated and the residue was purified by flash column chromatography (silica gel, EtOAc/hexane, 2/1) to give **10** (0.409 g) as a white semisolid. This solid was immediately dissolved in dry DMF (15 mL), treated with LiN_3 (0.137 g, 2.796 mmol), and the reaction mixture was heated to 80 °C under an atmosphere of argon for 12 h. After reaching ambient temperature, EtOAc (150 mL) was added and the resulting solution was extracted with brine (3 × 10 mL) and water until neutral pH. The organic layer was dried ($MgSO_4$), filtered, and concentrated to dryness. The residue was purified by flash column chromatography (silica gel, EtOAc/hexane, 1/1) to give **11** (0.233 g, 63%) as a white foam: mp 60−62 °C; IR (KBr) 2102 cm^{-1}; ^{1}H NMR ($CDCl_3$) δ 9.20 (s, 1 H, NH), 8.05−7.97 and 7.60−7.38 (m, 5 H, Ph), 7.09 (d, J < 1 Hz, 1 H, H-6), 4.60 (m, 2 H, $PhCOOCH_2$), 4.17 (d, J = 7.5 Hz, 1 H, H-3′), 2.60 (ddd, J = 13.8, 7.9, 1.91 Hz, 1 H, H-2′$_a$), 2.51 (irregular t, J ca. 7.5 Hz, H-4′),

2.15 (d, J = 13.8 Hz, 1 H, H-2′$_b$), 1.82 (d, J < 1 Hz, 3 H, CH_3), 1.78 (dd, J = 9.9, 4.9 Hz, 1 H, H-5′), 1.41 (irregular t, J ca. 5.5 Hz, 1 H, H-6′$_a$), 0.17 (m, 1 H, H-6′$_b$). Anal. Calcd for $C_{19}H_{19}N_5O_4 \cdot 0.25H_2O$: C, 59.13; H, 5.09; N, 18.15. Found: C, 59.13; H, 5.15; N, 17.89.

(1′*S*,3′*S*,4′*S*,5′*S*)-3′-Azido-4′-(hydroxymethyl)-1′-(5-methyl-2,4-(1*H*,3*H*)-dioxopyrimidin-1-yl)bicyclo[3.1.0]hexane (2). A stirred solution of **11** (0.208 g, 0.545 mmol) in MeOH (12 mL) was treated with K_2CO_3 (0.113 g, 0.818 mmol) and stirred at ambient temperature overnight. The reaction mixture was filtered, and the collected solid cake was washed with MeOH (3 × 5 mL). The collected filtrate was reduced to dryness, and the residue was purified by flash column chromatography (silica gel, gradient 1 → 5% MeOH/CH_2Cl_2) to give **2** (0.115 g, 76.2%), as a white solid: mp 199−201 °C (EtOAc); $[\alpha]_D$ = −64.3 (*c* 0.42; $CHCl_3$); IR (KBr) 2090 cm^{-1}; ^{1}H NMR ($CDCl_3$) δ 9.23 (br s, 1 H, NH), 7.13 (d, J = 1.1 Hz, 1 H, H-6), 4.49 (br d, J = 11.6 Hz, 1 H, OH), 4.20 (d, J = 7.7 Hz, 1 H, H-3′), 3.93 (d, J = 11.6 Hz, 1 H, C*H*OH), 3.75 (td, J = 11.3, 4.0 Hz, 1 H, CH*H*OH), 2.55 (ddd, J = 13.5, 7.8, 2.3 Hz, 1 H, H-2′$_a$), 2.23 (distorted t, 1 H, H-4′), 2.07 (d, J = 13.5 Hz, 1 H, H-2′$_b$), 1.90 (d, J = 1.1 Hz, 3 H, CH_3), 1.84 (dd, J = 9.7, 4.9 Hz, 1 H, H-5′), 1.35 (irregular t, J ca. 5.4 Hz, 1 H, H-6′$_a$), 1.05 (ddd, J = 9.7, 5.9, 2.3 Hz, 1 H, H-6′$_b$); ^{13}C NMR ($CDCl_3$) δ 12.29, 17.04, 28.89, 38.18, 48.77, 49.94, 63.66, 65.21, 112.02, 141.01, 151.58, 163.52; FABMS *m*/*z* (relative intensity) 278 (MH^+, 58), 127 (Thy + 2H, 13). Anal. Calcd for $C_{12}H_{15}N_5O_3 \cdot 0.5H_2O$: C, 50.34; H, 5.63; N, 24.46. Found: C, 50.44; H, 5.39; N, 24.35.

Synthesis of (N)-*methano*-Carba-AZT Triphosphate (3·$P_3O_8Na_4$) and (S)-*methano*-Carba-AZT Triphosphate (4·$P_3O_8Na_4$). Each starting carbocyclic nucleoside (0.016 g, 0.058 mmol) was dissolved in trimethyl phosphate (0.4 mL) and cooled to 0 °C under an atmosphere of argon. Phosphorus oxychloride (60 μL, 0.632 mmol) was added, and the solution was stirred for 3 h at 0 °C. The reaction mixture was removed from the ice bath and treated immediately with tri-*n*-butylamine (0.37 mL), tri-*n*-butylammonium pyrophosphate (1.0 g, 1.83 mmol) dissolved in dry diethylformamide (4 mL), and triethylammonium bicarbonate (TEAB) buffer (7.5 mL, 1 M, pH 8.5). The resulting mixture was stirred at ambient temperature for 1 h, concentrated to dryness, redissolved in water (50 mL), and reduced to dryness again under vacuum for 14 h. The residue was dissolved in TEAB (2 mL, 0.01 M) and applied to a chromatography column (Pharmacia DEAE Sephacel, 2 × 25 cm, TEAB 0.01 M buffer). Two linear gradients of TEAB (400 mL, 0.01 → 0.1 M) and (600 mL, 0.1 M → 0.6 M) were used in succession to elute the product. Major peaks absorbing at 254 and 280 nm were monitored using a Pharmacia dual-path UV monitor and collected. The identity of the triphosphates was confirmed by HPLC analysis performed as described below. The triphosphates were further purified by column chromatography (Analtech, bonded C-18, 35−75 μm, 1.75 × 10 cm, 0.01 M TEAB), and the product-containing fractions were lyophilized, dissolved in water, and eluted through a Dowex 50X8-100 (Na^+) ion-exchange resin (50 mL) with water. The corresponding sodium salts were obtained as white solids after lyophilization (0.010−0.015 g, 18−33%). Each sample was weighed accurately and brought to a volume of 1.0 mL (water, HPLC grade). HPLC analysis was performed with a Whatman Partisil 10 SAX (4.6 × 250 mm) anion-exchange column in a Waters WISP model 712 autosampler with two model 510 HPLC pumps and a Waters model 440 absorbance detector (at 254 nm) connected in series with a Waters model 994 photodiode array detector. The samples were eluted with a mobile phase initially of 0.01 M $(H_4N)H_2PO_4$, native pH, for 15 min followed by a 25-min linear gradient to 0.7 M $(H_4N)H_2PO_4$ with 10% MeOH (native pH), which was maintained for 5 min, finally returning to initial conditions in 6 min using a linear gradient. The column was allowed to equilibrate for 9 min prior to the next injection. Instrument control, data analysis, and data storage were accomplished using a Waters Millennum V2.1 chromatography software run on a NEC Image 466 PC. Under these conditions, the predominant peaks (area = 88.9−91.1%) eluted with a retention time comparable to that of authentic AZT triphosphate (t_R = 33.2−34.0 min). The amount of diphosphate (t_R = 24.5−25 min) was ca. 5%. Assuming a molecular weight of 624 (tetrasodium salt monohydrate) and a λ_{max} of 268 (ϵ = 9549), the purities (% by weight) of (N)-*methano*-carba-AZT triphosphate and (S)-*methano*-carba-AZT were 63.8% and 77%, respectively.

NMR Solution Conformation Experiments. The concentrations of all samples were between 20 and 36 mM dissolved in $CDCl_3$ or in mixtures of $CDCl_3$ and CD_3OD. All spectra were recorded on a Bruker AMX instrument at 500 MHz except for the 1D ^{13}C NMR spectra, which were recorded on a Bruker AC250 operating at 62.9 MHz. The temperature for data collection at 500 MHz was set to 25 °C and controlled by a Eurotherm variable-temperature unit. Phase-sensitive NOESY[21] spectra were collected with standard pulse sequences with a mixing time of 300 ms and a recycle delay of 2.5 s. Quadrature detection in f_1 was performed by time-proportional phase incrementation (TPPI).[22] NOEs obtained were positive (i.e., of opposite phase to the diagonal peaks), which proved that the extreme narrowing limit ($\omega t_c \ll 1$) was in effect for these small, rapidly tumbling molecules. Carbon assignments were made with the aid of HMQC[23] spectra recorded with and without decoupling for both **1** and **2**. 1D NOE spectra were obtained with the NOEMULT program in the Bruker UXNMR software. Multiple points on each resonance were irradiated for a total of 2 s, and each scan was preceded by a recycle delay of 4 s. A total of 8 scans/experiment were collected, and the data was interleaved for 16−32 cycles. The time domain data of an off-resonance irradiated dataset was subtracted with that of a FID from a dataset with an irradiated resonance, and the resulting difference was multiplied with an exponential function (line broadening = 0.5) and Fourier transformed. Integrations were performed by comparing the height of the irradiated peak in the difference spectrum (set to 100%) with that of the enhanced peaks. The errors were estimated to be on the order of ±1% by measuring the height of extraneous peaks present that did not show real NOEs.

HIV-1 Reverse Transcriptase Assay. Inhibitory activity of compounds against RT was determined as previously described.[24,25] Two different RT preparations were employed: (i) a recombinant RT from a wild-type virus (RT_{BH10}) and (ii) a preparation of disrupted virions of HIV-1_{LAI} (a mixture of HIV strains).[24] Briefly, concentrations ranging from 0.001 to 1 μM of the triphosphate inhibitors were added to reaction mixtures (50 μL) containing poly(rA)·$(dT)_{12-18}$, 50 mM Tris-HCl (pH 8), 6 mM $MgCl_2$, 0.06% Triton X-100, and 10 μM [^{3}H]TTP with 8 nM RT_{BH10} and 20 μM [^{3}H]TTP with RT from HIV_{LAI}. The reaction was initiated by raising the temperature of the mixtures from 0° to 37 °C followed by a 30-min incubation at 37 °C. Reactions were quenched by the addition of a chilled solution of 10X TCA and 20 mM pyrophosphate, and reaction mixtures were spotted onto Whatman GF/C filters on a Millipore vacuum apparatus. The filters were washed five times with the TCA solution to remove excess nucleotides and 2 times with EtOH to allow for drying. The amount of [^{3}H]TMP incorporated into DNA and absorbed on the filter was determined using a scintillation counter. Results are expressed as DPM of [^{3}H]TMP incorporated/50 μL reaction mixture. All assays were performed in triplicate.

Acknowledgment. This paper is dedicated to Professor Victor M. Marquez Antich of the Faculty of Pharmacy, Universidad Central de Venezuela, on the occasion of his 80th birthday. The authors wish to express their appreciation to Drs. John S. Driscoll and David G. Johns for their helpful insights and support of this project.

Supporting Information Available: Tables of crystal data and structure refinements, atomic coordinates, bond distances and angles, and anisotropic thermal parameters for compound **2** (7 pages). See any current masthead page for ordering and Web access instructions.

JA973535+

(21) Macura, S.; Ernst, R. R. *Mol. Phys.* **1980**, *41*, 95.
(22) Rance, M.; Sorenson, O. W.; Bodenhausen, G.; Wagner, G.; Ernst, R. R.; Wuthrich, K. *Biochem. Biophys. Res. Commun.* **1983**, *117*, 479.
(23) Bax, A.; Davis, D. G. *J. Magn. Reson.* **1985**, *65*, 355.
(24) Mitsuya, H.; Weinhold, K. J.; Furman, P. A.; St. Clair, M. H.; Lehrman, S. N.; Gallo, R. C.; Bolognesi, D.; Barry, D. W.; Broder, S. *Proc. Natl. Acad. Sci. U.S.A.* **1985**, *82*, 7096.
(25) Ueno, T.; Shirasaka, T.; Mitsuya, H. *J. Biol. Chem.* **1995**, *270*, 23605.